Taylor & Francis
Taylor & Francis Group

Philosophical Magazine

ISSN: 1478-6435 (Print) 1478-6443 (Online) Journal homepage: http://www.tandfonline.com/loi/tphm20

Externally applied stress sign and film elastic properties effects on brittle film fracture

Tao Guo, Xiaolu Pang, Yeting Xi, Alex A. Volinsky & Lijie Qiao

To cite this article: Tao Guo, Xiaolu Pang, Yeting Xi, Alex A. Volinsky & Lijie Qiao (2016) Externally applied stress sign and film elastic properties effects on brittle film fracture, Philosophical Magazine, 96:5, 447-458, DOI: 10.1080/14786435.2015.1132018

To link to this article: http://dx.doi.org/10.1080/14786435.2015.1132018

PHILOSOPHICAL MAGAZINE, 2016
VOL. 96. NO. 5, 447–458
http://dx.doi.org/10.1080/14786435.2015.1132018

Taylor & Francis
Taylor & Francis Group

Externally applied stress sign and film elastic properties effects on brittle film fracture

Tao Guo[a], Xiaolu Pang[b], Yeting Xi[b], Alex A. Volinsky[c] and Lijie Qiao[a]

[a]Key Laboratory for Environmental Fracture (MOE), Corrosion and Protection Center, University of Science and Technology Beijing, Beijing, China; [b]Department of Materials Physics and Chemistry, University of Science and Technology Beijing, Beijing, China; [c]Department of Mechanical Engineering, University of South Florida, Tampa, FL, USA

ABSTRACT

Rectangular stainless steel samples with TiN film deposited on the front lateral surface were loaded in three-point bending to the maximum normal strain of 6%. Scanning electron microscopy showed that vertical cracks appeared in the tension zone when the tensile strain exceeded 1.5%, while horizontal cracks appeared in the compression zone when the compressive strain exceeded –2.9%. Film cracks in the compressive zone originate from the tensile stress imposed by the plastically deformed substrate due to the Poisson's expansion. Taking plastic deformation and Poisson's expansion of the substrate in compression into account, theoretical analysis of normal stress distribution along the cracked film segment in compression is presented. Substrate strain and film elastic properties affect film cracking in the compressive zone. At larger compressive strain, some transverse cracks along with buckling cause the film spallation. The presented method is useful for studying brittle film fracture with variable strain levels in a single sample.

ARTICLE HISTORY
Received 16 October 2015
Accepted 10 December 2015

KEYWORDS
Bending; compression; cracking; deposition; thin films; fracture; thin-film mechanics; TiN film; stainless steel substrate; Poisson's expansion

1. Introduction

Brittle films are widely used in various applications, including surface modification protective coatings [1], passivation dielectric layers in semiconductor devices [2] and negative electrodes in lithium batteries [3]. In service, these films can be subjected to stresses due to temperature and humidity fluctuations [4,5] and external loads [6,7]. Brittle films can crack at low strain due to quite low fracture toughness [8], leading to the whole device or system failure [9]. Cracking is one of the most common failures of thin brittle films and has been extensively studied using various methods, including indentation [10,11], uniaxial tension [12–15], bending [7,16] and finite-element modelling [17,18]. These experiments focused on the tensile stress effects on the film fracture behaviour. Affected by preparation technology and service environment, thin films can be exposed to compressive stresses [4,8]. Large compressive stress combined with insufficient adhesion at the interface often lead

CONTACT Xiaolu Pang pangxl@mater.ustb.edu.cn

to local or global film detachment and buckling [19]. Until now, only few researchers have conducted systematic studies of the compressive stress effects on film fracture behaviour, including residual stress after annealing [4,6] and external stress under compression [20,21].

Some studies have shown that the state of the compressive stress in the film changes and becomes tensile in some areas, inducing film cracking, despite the overall compressive stress [22,23]. Transverse stress arises in the film under uniaxial tension due to a mismatch of the Poisson's ratios between the thin films and the substrate leading to transverse contractions [14,24,25]. Therefore, film tensile strain $\varepsilon_{y,f}$ will be expected to appear in the compressive zone, perpendicular to the externally applied compressive strain, $\varepsilon_{x,s}$, because of the Poisson's expansion. Here, a new method to study fracture behaviour of a brittle film in compression is presented. When a ductile substrate with a brittle film on the lateral surface is bent, both external normal tensile and compressive stresses are present in the film simultaneously, depending on the position with respect to the neutral axis. Fracture of a brittle film under tensile and compressive stress can be studied simultaneously to compare the two types of fracture behaviour.

The key factors which can affect film cracking and stress distribution with two parallel film cracks under externally applied tensile stress have been studied experimentally and theoretically [12,15,18,26]. However, under compression, no theoretical analysis has been established to explain the film cracking, except for Xue et al., who simulated the process of film buckling and transverse cracking with interfacial delamination [20]. Therefore, the aim of this paper is to analyze the conditions of cracks forming in the film and obtain the stress distribution around the two parallel cracks in the compressive zone.

2. Experimental procedure

The dimensions of the 304 stainless steel substrates were 15.5 mm × 6 mm × 1.5 mm. TiN films were deposited on the front 15.5 mm × 1.5 mm surface (lateral surface). The TiN films were deposited at 300 °C by reactive RF-pulsed magnetron sputtering in an industrial physical vapour deposition system. The 304 steel substrates were rotated in front of the titanium target with the 76 mm diameter. Nitrogen gas flow during deposition was 1.2 cm^3/min, while argon flow was 30 cm^3/min. The base pressure in the sputtering chamber was less than 5×10^{-3} Pa, and the deposition pressure was 0.3 Pa, while the Ar pressure was 0.25 Pa. During the sputter deposition the bias of –80 V was applied to the substrate. The target power was 300 W, and the deposition rate was 7 nm/min.

The surface microstructure of the TiN film on the 304 stainless steel is shown in Figure 1(a). The average surface roughness in the 40 μm × 40 μm area is about 80 nm, measured by atomic force microscopy (AFM, Veeco Dimension V). In order to conveniently observe the cross-sectional microstructure of the TiN film, it was deposited in silicon substrate with the same deposition parameters as for the 304 SS substrates. As seen in Figure 1(b), TiN film has large parallel columnar grains, which is similar to results on the steel substrate [27], and the film thickness is about 1.3 μm. The residual tensile stress of 180 MPa in the TiN film was measured by means of the XRD $(\cos \alpha \sin \Psi)^2$ method. Young's modulus of the film, E_f, was measured by nanoindentation (TI900, Hysitron) as $E_{f(TiN)}$ = 220 GPa, using Berkovich tip with an effective tip radius of 150 nm. The indenter displacement into the film was about 120 nm, less than 1/10 of the film thickness, thus the substrate had no significant effects on the film Young's modulus measurements [28]. Poisson's ratio of the

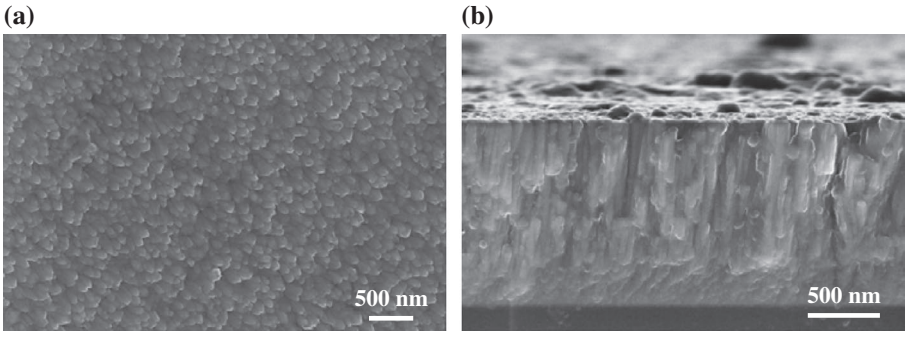

Figure 1. Microstructure of the TiN film: (a) The surface morphology of TiN film on 304 SS steel substrate; (b) The cross-sectional microstructure of TiN film on silicon substrate.

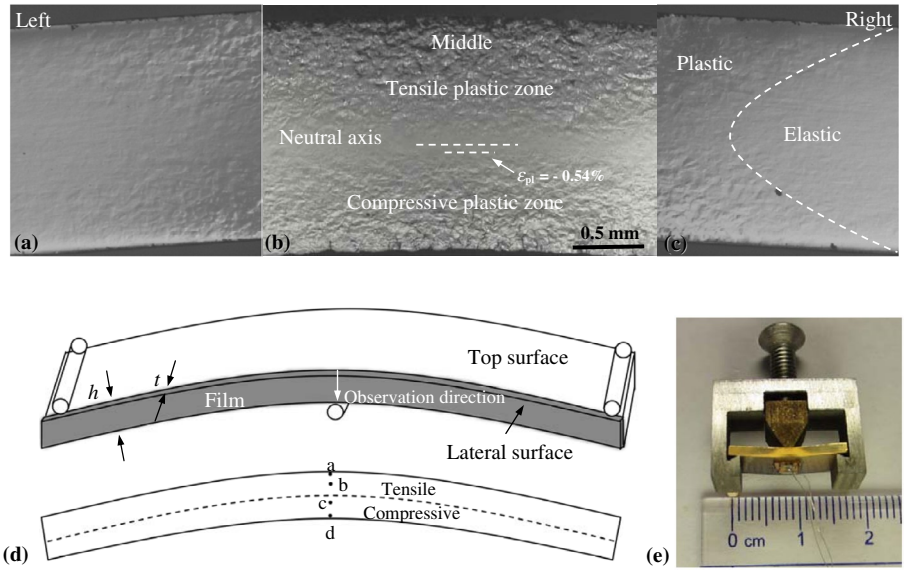

Figure 2. Polarized light optical microscope images of the sample after bending: (a) left boundary of the plastic zone; (b) middle of the plastic zone; (c) right boundary of the plastic zone; (d) Schematics of the sample in three-point bending. The film is on the lateral surface is labelled by grey colour. The sites for observing the crack density under SEM are labelled as a, b, c and d; (e) Image of the sample in the three-point bending device.

TiN film, $\nu_{f(\mathrm{TiN})}$, is 0.25 [29]. The stainless steel bar with TiN film on the front lateral surface (15.5 mm × 1.5 mm) was bent with a strain rate of $2 \cdot 10^{-2}$ s^{-1} to the maximum strain of 6%, using wedge with radius of 0.75 mm along the width of the bar by a custom-made device. Polarized light optical microscope images show plastic deformation of the lateral surface in Figure 2(a)–(c). 304 stainless steel Substrates with TiN films on the front lateral surface were bent to the maximum strain of 6% and examined in SEM along the *abcd* direction, as shown schematically in Figure 2(d). The maximum strain on the top sample surface was measured using a strain gauge in Figure 2(e).

Assuming that the externally applied moment is constant along the same longitude, the strain can be calculated, as follows:

$$\varepsilon_x(y) = \frac{2y}{h}\varepsilon_{\text{top}} \tag{1}$$

where h is the substrate thickness and y is the distance from the neutral axis. Based on the 304 stainless steel tensile test, the critical plastic strain of the substrate, ε_{pl}, is 0.54%. The maximum normal strain close to the sample top and bottom surfaces in Figure 2(b) is ±6%.

3. Results and discussion

Stainless steel 304 substrates with TiN films on the front lateral surface were bent to the maximum strain of 6% and examined in SEM along the *abcd* direction, as shown schematically in Figure 2(d). Based on Equation (1), the strain at the four sites can be obtained by measuring the distance to the sample edge using SEM. The site *a* is near the top of the sample with $\varepsilon = 6\%$, and many vertical cracks and spallation appear in the film with almost the same distance between them, as seen in Figure 3(a). The strain decreased from $\varepsilon = 6\%$ at the site *a* to $\varepsilon = 1.5\%$ at the site *b*, and the crack density decreased, until cracks arrested at the bottom of Figure 3(b). In the compression zone, transverse cracks with almost the same distance between them, which are normal to the vertical cracks in the tension zone, appear when the compressive strain is larger than –2.9%, as seen in Figure 3(c), corresponding to the site *c* in Figure 2(d). These transverse cracks are similar to the tension cracks. When the compressive strain increases from –2.9 to –6%, some transverse cracks initiate from the imperfections upon buckling, causing different distance between them, as seen in Figure 3(d). Therefore, the critical compressive strain for transverse crack initiation in the compression zone is about –2.9%, which is much larger than the critical tensile strain of vertical crack initiation in the tension zone. The crack density increased quickly in the initial loading stage and then saturated gradually to almost the same crack density both in tension and compression, as shown in Figure 3(e).

Under tension, as shown in Figure 3(a) and (b), cracking behaviour of thin brittle films on ductile substrates can generally be comprehended by the shear lag model, as the minimum and the maximum crack spacings are off by a factor of two or less than two [30]. The normal stress in the substrate is transferred to the coating by the interface. It is found both experimentally and theoretically that the tensile stress is maximum at the mid-point and minimum near the edges of the film attached segment [6,12,14,26,30,31]. When the stress exceeds the fracture stress, cracks will initate in the middle of the attached film segment, leading to the same parallel cracks spacing, as seen in Figure 3(b). Initially, the crack spacing is large and the stress distribution reaches a plateau [13,14,26]. At higher strain, the crack spacing becomes smaller, and the stress distribution in the attached film segment is parabolic in shape [13,26,32]. When the crack density becomes saturated, the interfacial shear stress approaches a critical value to delaminate the film [13,30]. The initiation of cracks releases the tensile stress in the film by the formation of the shear lag [16]. Hence, higher strain is required for further cracking, as shown in Figure 3(b). At larger strain additional cracks will form upon buckling [22], causing film spallation seen in Figure 3(a).

Under compression, in the previous studies of for ductile films, the transverse cracks grow behind delaminated buckles [20,21]. However, for the TiN film, the transverse cracks appear

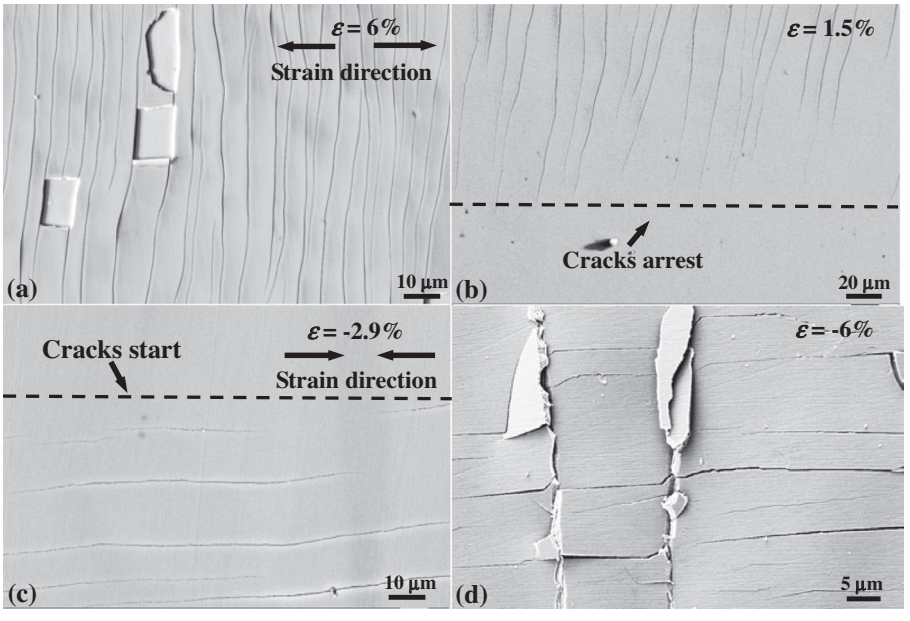

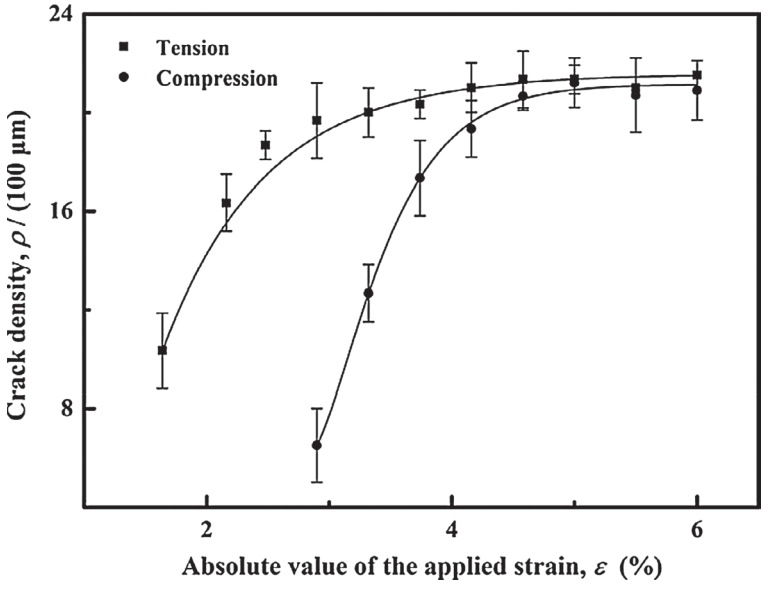

Figure 3. Scanning electron micrograph of the samples: (a) with the maximum tensile strain $\varepsilon = 6\%$ and many vertical cracks with spallation; (b) $\varepsilon = 1.5\%$ with a few vertical cracks on the top and no cracks on the bottom of the image; (c) $\varepsilon = -2.9\%$ with no cracks on the top and a few transverse cracks with the same crack spacing on the bottom of the image; (d) Maximum compressive strain $\varepsilon = -6\%$ with many transverse cracks and delaminations; (e) Average crack density as a function of the absolute value of the applied strain both in tension and compression.

prior to buckling at small compressive strain, as shown in Figure 3(c). Therefore, it couldn't be interpreted that the transverse cracks are induced simply by buckling as demonstrated in previous work. Before buckles appear, the transverse cracks in compression are induced

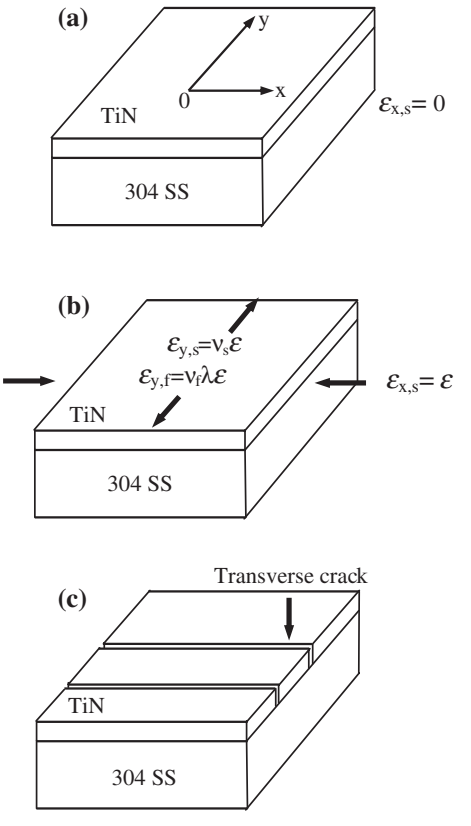

Figure 4. Schematics of the substrate Poisson's expansion effects on the film under compressive zone: (a) Without applied strain; (b) At small compressive strain ε along the *x*-direction. The strains in the film and the substrate along the *y*-direction are $\nu\lambda\varepsilon$ ($\lambda < 1$) and ν, respectively. For brittle film and ductile substrate system, $\nu_s > \nu_f$; (c) Transverse cracks appear at large compressive strain due to the Poisson's expansion.

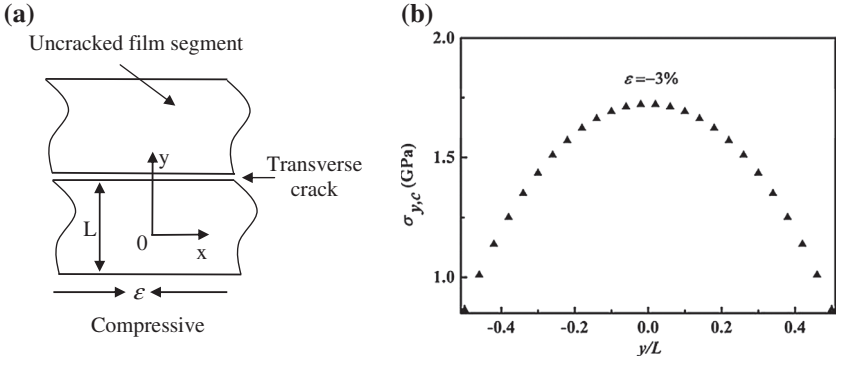

Figure 5. Coordinate system and crack schematics for: (a) Compression; (b) Stress distribution along the cracked film segment in the compressive zone, where the stress is the maximum in the middle of the attached film segment.

by the Poisson's expansion effect. As illustrated in the Figure 4, film tensile strain along the y-direction, $\varepsilon_{y,f}$, is expected to arise in the compressive zone, perpendicular to the externally applied compressive strain, $\varepsilon_{x,s}$. That is to say the transverse cracks in the compressive zone are induced by the tensile stress. In addition, the transverse cracks have almost the same distance between them when they start to appear, as seen in Figure 3(c). Hence, the shear lag model is also suitable at the initial stage in compression.

Here, a modification of the shear lag model in compression is presented to consider the effects of plastic deformation of the substrate. Most of the analysis is based on the stress distribution in the tensile zone [13], but taking Poisson's expansion of the substrate in compression into account. The coordinate system origin is located in the middle of the two transverse cracks in the compression zone with the y-axis perpendicular to the cracks, as shown schematically in Figure 5(a). The distance between the two cracks is L, and the stress distribution region is $-L/2 \le y \le L/2$. The applied strain is compressive along the x-direction and the film is under biaxial residual stress, σ_{res}, before bending. Plane strain conditions are taken into account here. In addition, when the system has an infinite length in the x-direction, there is no stress variation along the x-direction. First, let's assume that the substrate deformation due to external loading is uniform and elastic, while the interfacial shear stress is also linear elastic. According to Frank et al. [14], one can obtain a displacement equation between the two cracks in the film:

$$\frac{\partial^2 u_{y,f}}{\partial y^2} = \frac{1}{\xi^2}\left(u_{y,f} - u_{y,s}\right) \tag{2}$$

where u_y is the displacement along the y-direction, while the subscripts f and s represent the film and the substrate, respectively. $\xi = \sqrt{E_f t / G_{\text{int}}\left(1-\nu_f^2\right)}$ is the stress transfer length, where E_f is the Young's modulus of the film and t is the thickness of the film, while G_{int} is the shear modulus of the interface. It is assumed that the stress transfer length, ξ, is constant in this analysis. The displacement of the substrate in the y-direction, $u_{y,s}$, is given as $u_{y,s} = \varepsilon_{y,s} y = -\nu_s \varepsilon_{\text{app}} y$ with the macroscopically applied strain ε_{app}. Equation (2) can be also written as follows:

$$\frac{\partial^2 u_{y,f}}{\partial y^2} = \frac{1}{\xi^2}\left(u_{y,f} + \nu_s \varepsilon_{\text{app}} y\right) \tag{3}$$

In the compression zone, the boundary conditions are $\sigma_{y,f}\left(y = \pm L/2\right) = 0$ due to the stress release by forming cracks and $u_{y,f}\left(y = 0\right) = 0$ in the centre of the two cracks because of the displacement symmetry. The solution of Equation (3) with respect to the boundary condition $u_{y,f}\left(y = 0\right) = 0$ is:

$$u_{y,f} = K \sinh\left(y/\xi\right) - \nu_s \varepsilon_{x,f} y \tag{4}$$

where K is a constant and $\varepsilon_{x,f}$ is equal to the applied strain ε_{app}, which is negative (compressive). The total stress in the film is given by superposition of the elastic stress $\sigma_{y,f}^{\text{el}}$, caused by the three-point bending and the biaxial residual stress, σ_{res}, which is constant during the film cracking progress:

$$\sigma_{y,f} = \sigma_{y,f}^{\mathrm{el}} + \sigma_{\mathrm{res}} \tag{5}$$

Considering that the stress is homogeneous and isotropic, according to the Hooke's law, the elastic stress in the film can be expressed as follows:

$$\sigma_{y,f}^{\mathrm{el}} = \frac{E_f}{1-\nu_f^2}\left(\varepsilon_{y,f} + \nu_f \varepsilon_{\mathrm{app}}\right) \tag{6}$$

Combining Equations (5) and (6), and taking the boundary condition $\sigma_{y,f}\left(y = \pm L/2\right) = 0$ into account, one finds:

$$\varepsilon_{y,f}(y = \pm L/2) = -\nu_f \varepsilon_{\mathrm{app}} - \sigma_{\mathrm{res}}\left(1-\nu_f^2\right)/E_f \tag{7}$$

Since $\varepsilon_{y,f} = \partial u_{y,f}/\partial y$, differentiating Equation (3) and using the value of $\varepsilon_{y,f}\left(y = \pm L/2\right)$, the strain in the cracked segment along the y-direction can be expressed as follows:

$$\varepsilon_{y,f} = \left[\left(\nu_s - \nu_f\right)\varepsilon_{\mathrm{app}} - \varepsilon_{\mathrm{res}}\right]\frac{\cosh\left(y/\xi\right)}{\cosh\left(L/2\xi\right)} - \nu_s \varepsilon_{\mathrm{app}} \tag{8}$$

where $\varepsilon_{\mathrm{res}}$ is the residual strain, $\varepsilon_{\mathrm{res}} = \left(1-\nu_f^2\right)\sigma_{\mathrm{res}}/E_f$. Using Equations (4), (6), (7) and (8), one can give the expression for the normal stress in the compression zone in the film, $\sigma_{y,f}$:

$$\sigma_{y,f} = \frac{E_f}{1-\nu_f^2}\left[\varepsilon_{\mathrm{res}} - \left(\nu_s - \nu_f\right)\varepsilon_{\mathrm{app}}\right]\left[1 - \frac{\cosh\left(y/\xi\right)}{\cosh\left(L/2\xi\right)}\right] \tag{9}$$

The analysis is based on the assumption that the interfacial shear stress transfer is linear elastic and the substrate deformation is elastic, but does not consider plasticity effects of the substrate. However, based on the 304 stainless steel tensile test results, plastic deformation takes place when the strain is about ±0.54%, as shown in Figure 2(b). Before yielding, the applied strain is transferred to the coating by the shear stress at the interface as discussed above. Once the substrate yields, the plastic strain in the substrate is transferred to the film, which can be expressed as follows: $\varepsilon_{\mathrm{pl},f}^{*} = \left(\nu_s - \nu_f\right)\left(-\varepsilon_{\mathrm{app}} - \varepsilon_{\mathrm{el}}\right)$. Then the stress is:

$$\sigma_{\mathrm{pl},f}^{*} = \frac{E_f}{1-\nu_f^2}\left(\nu_s - \nu_f\right)\left(-\varepsilon_{\mathrm{app}} - \varepsilon_{\mathrm{el}}\right) \tag{10}$$

where $\varepsilon_{\mathrm{el}}$ is the elastic strain of the substrate. The total stress in the film is the sum of $\sigma_{y,c}$ and $\sigma_{\mathrm{pl},f}^{*}$, i.e.:

$$\sigma_{y,f}^{*} = \frac{E_f}{1-\nu_f^2}\left[\varepsilon_{\mathrm{res}} - \left(\nu_s - \nu_f\right)\varepsilon_{\mathrm{el}}\right]\left[1 - \frac{\cosh\left(y/\xi\right)}{\cosh\left(L/2\xi\right)}\right] + \frac{E_f}{1-\nu_f^2}\left(\nu_s - \nu_f\right)\left(-\varepsilon_{\mathrm{app}} - \varepsilon_{\mathrm{el}}\right) \tag{11}$$

Based on Equation (11), the cracks in compressive zone are caused by lateral contraction mismatch of the film and the substrate, due to the Poisson's expansion of the substrate. However, the crack in the tensile zone is determined by the macroscopically applied strain.

Hence, larger strain is needed to initiate cracks in the compressive zone, as shown in Figure 3(e). Equation (11) is only suitable for brittle films without plastic deformation. For a ductile film, large plastic deformation would take place prior to fracture since it could undergo yielding. As demonstrated by Equation (11), the first term is elastic and contributes very little to the total stress, since the elastic strain in the substrate is very small. The major contribution is the second plastic term. The cracking in the brittle film was primarily induced by the substrate plastic strain. After the substrate yields, the normal stress in the substrate is equal to the yield stress, and does not increase further (strain hardening is not taken into account here). However, the substrate continues to plastically strain further. For a stainless steel substrate, when the applied strain exceeds the yield strain, the plastic Poisson's ratio is about 0.5, rather than the elastic Poisson's ratio of 0.29. Based on Equation (11) with σ_{res} = 0.18 GPa, ε_{el} = 0.54%, E_f = 220 GPa and ν_s = 0.5 in the plastic zone of the substrate, Figure 5(b) shows the stress distribution along the y-direction in the cracked film segment for the applied compressive strain of ε_{app} = –3%. As illustrated in Figure 5(b), the critical stress of the transverse crack initiating in the compression zone is about 1.7 GPa, and when the external compressive strain is ε_{app} (–2.9%, the film would crack at the middle of the attached segment.

Krishnamurthy and Reimanis [15] made a comparison between the FE-generated stress distribution profiles on the surface of the CrN coating on brass. They found that a simple shear lag model cannot describe the complex stress state at and near the edges of the cracked coating segment. In the FE modelling, a large compressive stress is found near the cracked segment edge, which is not described by the shear lag model. The complex stress transitions at and near the crack boundaries are currently not taken into account. The analysis is presented just to reveal the reason why the film cracks in the compressive zone. In addition, the stress gradient due to the three-point bending itself has not been taken into account here. The stress difference is about 70 MPa when the vertical crack spacing is about 5 μm, which can be ignored compared with the much larger local film stress.

However, as the applied compressive strain increases, the stress along the x-direction exceeds the adhesion strength of the TiN film, and it starts to buckle, thus Equation (11) is not suitable for this case. Buckling indicates that the film debonds from the substrate and becomes freestanding. Freestanding films commonly crack at a much lower strain than the fully bonded films [33]. As a consequence, some transverse cracks initiate from the imperfections upon buckling because of the tensile stress along the vertical y-direction. Then, they grow down along the buckle width direction towards the interface. When the transverse cracks are present, the accumulation of shear stresses near the free edges motivates interfacial failure, which will eventually lead to film delamination and spallation, as shown in Figure 3(d). In addition, the transverse cracks initiating from the imperfections upon buckling could give rise to the tensile stress relaxation of the film along the y-direction. This will cause transverse cracks, which should be formed in the middle of the missing segment. Therefore, the crack density both in tension and compression is almost the same, as seen in Figure 3(e). At large compressive strain, the transverse cracks are induced not only by the Poisson's expansion effect, but also by buckling. These two factors contribute to the transverse cracks occurrence. Although the crack spacing does not satisfy the shear lag theory, where the ratio between the maximum and the minimum crack spacing is about 2 [30], the shear lag model can be used for the discussion why the film cracks parallel to the applied stress in the compressive zone.

4. Conclusions

In summary, a comprehensive study of the influence of tensile/compressive stress and elastic properties of the film on cracking was performed. Experimental results and analysis allowed the following conclusions to be drawn.

(1) For the 304 stainless steel bent sample with the TiN film on one lateral surface, vertical cracks appear in the tensile zone when the tensile strain $\geq 1.5\%$ and the transverse cracks exist in the compressed zone when the compressive strain is $\geq -2.9\%$.
(2) Transverse cracks along with buckling could cause TiN film spallation in the compressive zone.
(3) The Poisson's expansion of the substrate, elastic properties, residual stress of the film and buckling could contribute to the transverse cracking of the film in the compressive zone.

The presented method allows studying brittle film fracture on ductile substrates with variable strain levels in a single bending experiment.

Disclosure statement

No potential conflict of interest was reported by the authors.

Funding

This work was supported by the National Natural Science Foundation of China [grant number 51271022], [grant number 51431004]; Beijing Higher Education Young Elite Teacher Project [YETP0353]; National Basic Research Program of China [2012CB937502]; the National Science Foundation [IRES 1358088].

ORCID

Alex A. Volinsky http://orcid.org/0000-0002-8520-6248

References

[1] Z. Chen, L.Y.L. Wu, E. Chwa, and O. Tham, *Scratch resistance of brittle thin films on compliant substrates.* Mater. Sci. Eng. A 493 (2008), pp. 292–298.
[2] S.P. Tiwari, P. Srinivas, S. Shriram, N.S. Kale, S.G. Mhaisalkar, and V. Ramgopal Rao, *Organic FETs with HWCVD silicon nitride as a passivation layer and gate dielectric,*Thin Solid Films 516 (2008), pp. 770–772.
[3] X. Xiao, P. Liu, M.W. Verbrugge, H. Haftbaradaran, and H. Gao, *Improved cycling stability of silicon thin film electrodes through patterning for high energy density lithium batteries*, J. Power Sources 196 (2011), pp. 1409–1416.
[4] S.H. Jen, J.A. Bertrand, and S.M. George, *Critical tensile and compressive strains for cracking of Al2O3 films grown by atomic layer deposition,* J. Appl.Phys. 109 (2011), p. 084305.
[5] K.W. McElhaney and Q. Ma, *Investigation of moisture-assisted fracture in SiO_2 films using a channel cracking technique*, Acta Mater. 52 (2004), pp. 3621–3629.
[6] C. Chaiwong, D.R. McKenzie, and M.M.M. Bilek, *Cracking of titanium nitride films grown on polycarbonate*, Surf. Coat. Technol. 201 (2007), pp. 5596–5600.
[7] Y. Li, X.-S. Wang. and X.-K. Meng, *Buckling behavior of metal film/substrate structure under pure bending*, Appl. Phys. Lett. 92 (2008), p. 131902.

[8] L. Zhang, H. Yang, X. Pang, K. Gao, and A.A. Volinsky, *Microstructure, residual stress, and fracture of sputtered TiN films*, Surf. Coat. Technol. 224 (2013), pp. 120–125.
[9] T. Guo, L. Qiao, X. Pang, and A.A. Volinsky, *Brittle film-induced cracking of ductile substrates*, Acta Mater. 99 (2015), pp. 273–280.
[10] J.M. Jungk, B.L. Boyce, T.E. Buchheit, T.A. Friedmann, D. Yang, and W.W. Gerberich, *Indentation fracture toughness and acoustic energy release in tetrahedral amorphous carbon diamond-like thin films*, Acta Mater. 54 (2006), pp. 4043–4052.
[11] S. Math, S. Suresha, V. Jayaram, and S. Biswas, *Indentation of a hard film on a compliant substrate: film fracture mechanisms to accommodate substrate plasticity*, J. Mater. Sci. 41 (2006), pp. 7830–7837.
[12] F. Ahmed, K. Bayerlein, S.M. Rosiwal, M. Göken, and K. Durst, *Stress evolution and cracking of crystalline diamond thin films on ductile titanium substrate: Analysis by micro-Raman spectroscopy and analytical modelling*, Acta Mater. 59 (2011), pp. 5422–5433.
[13] B.F. Chen, J. Hwang, I.F. Chen, G.P. Yu, and J.H. Huang, *A tensile-film-cracking model for evaluating interfacial shear strength of elastic film on ductile substrate*, Surf. Coat. Technol. 126 (2000), pp. 91–95.
[14] S. Frank, U.A. Handge, S. Olliges, and R. Spolenak, *The relationship between thin film fragmentation and buckle formation: Synchrotron-based in situ studies and two-dimensional stress analysis*, Acta Mater. 57 (2009), pp. 1442–1453.
[15] S. Krishnamurthy and I. Reimanis, *Multiple cracking in CrN and Cr2N films on brass*, Surf. Coat. Technol. 192 (2005), pp. 291–298.
[16] Q.P. Cao, Y. Ma, Y. Xu, L.Y. Chen, C. Wang, Y.Y. Ruan, X.D. Wang, and J.Z. Jiang, *Bending behavior of electrodeposited glass Pd-P and Pd-Ni-P thin films*, Scr. Mater. 68 (2013), pp. 455–458.
[17] S. Nekkanty, M. Walter, and R. Shivpuri, *A cohesive zone finite element approach to model tensile cracks in thin film coatings*, J. Mech. Mater. Struct. 2 (2007), pp. 1231–1247.
[18] C. Xie and W. Tong, *Cracking and decohesion of a thin Al_2O_3 film on a ductile Al-5%Mg substrate*, Acta Mater. 53 (2005), pp. 477–485.
[19] S.-J. Yu, M.-G. Chen, J. Chen, H. Zhou, Y.-J. Zhang, and P.-Z. Si, *Spatial and kinetic evolutions of telephone cord buckles*, Surf. Coat. Technol. 228 (2013), pp. 258–265.
[20] X. Xue, S. Wang, C. Zeng, H. Bai, L. Li, and Z. Wang, *Buckling-delamination and cracking of thin titanium films under compression: Experimental and numerical studies*, Surf. Coat. Technol. 244 (2014), pp. 151–157.
[21] B. Cotterell and Z. Chen, *Buckling and cracking of thin films on compliant substrates under compression*, Int. J. Fract. 104 (2000), pp. 169–179.
[22] M. He, A. Evans, and J. Hutchinson, *The ratcheting of compressed thermally grown thin films on ductile substrates*, Acta Mater. 48 (2000), pp. 2593–2601.
[23] V.K. Tolpygo, J.R. Dryden, and D.R. Clarke, *Determination of the growth stress and strain in α-Al_2O_3 scales during the oxidation of Fe-22Cr-4.8Al-0.3Y alloy*, Acta Mater. 46 (1998), pp. 927–937.
[24] M.J. Cordill, F.D. Fischer, F.G. Rammerstorfer, and G. Dehm, *Adhesion energies of Cr thin films on polyimide determined from buckling: Experiment and model*, Acta Mater. 58 (2010), pp. 5520–5531.
[25] P.A. Gruber, J. Böhm, F. Onuseit, A. Wanner, R. Spolenak, and E. Arzt, *Size effects on yield strength and strain hardening for ultra-thin Cu films with and without passivation: A study by synchrotron and bulge test techniques*, Acta Mater. 56 (2008), pp. 2318–2335.
[26] C.H. Hsueh and M. Yanaka, *Multiple film cracking in film/substrate systems with residual stresses and unidirectional loading*, J. Mater. Sci. 38 (2003), pp. 1809–1817.
[27] S. Bhowmick, V. Jayaram, and S. Biswas, *Deconvolution of fracture properties of TiN films on steels from nanoindentation load-displacement curves*, Acta Mater. 53 (2005), pp. 2459–2467.
[28] E. Berasategui and T. Page, *The contact response of thin SiC-coated silicon systems-characterisation by nanoindentation*, Surf. Coat. Technol. 163–164 (2003), pp. 491–498.
[29] Matweb. Available at http://www.matweb.com[13.07.10].

[30] D.C. Agrawal and R. Raj, *Measurement of the ultimate shear strength of a metal-ceramic interface*, Acta Metall. 37 (1989), pp. 1265–1270.
[31] U.A. Handge, *Analysis of a shear-lag model with nonlinear elastic stress transfer for sequential cracking of polymer coatings*, J. Mater. Sci. 37 (2002), pp. 4775–4782.
[32] B.F. Chen, J. Hwang, G.P. Yu, and J.H. Huang, *In situ observation of the cracking behavior of TiN coating on 304 stainless steel subjected to tensile strain*, Thin Solid Films 352 (1999), pp. 173–178.
[33] T. Li, Z.Y. Huang, Z.C. Xi, S.P. Lacour, S. Wagner, and Z. Suo, *Delocalizing strain in a thin metal film on a polymer substrate*, Mech. Mater. 37 (2005), pp. 261–273.